



# GNSS-Denied Architecture for Unmanned Aerial Systems: From Classical Inertial Navigation to Drift-Free Performance

- Laura Train García**  PhD Candidate, Escuela Superior de Ingeniería Aeronáutica y del Espacio (ET-SIAE), Universidad Politécnica de Madrid, Spain. [l.train@alumnos.upm.es](mailto:l.train@alumnos.upm.es)  
Navigation Engineer, UAV Navigation - Grupo Oesia, San Sebastián de los Reyes (Madrid), Spain. [ltrain@uavnavigation.com](mailto:ltrain@uavnavigation.com)
- Miguel Ángel de Frutos Carro**  Managing Director and CTO, UAV Navigation - Grupo Oesia, San Sebastián de los Reyes (Madrid), Spain. [mfrutos@uavnavigation.com](mailto:mfrutos@uavnavigation.com)
- José María Pulido Fernández** Navigation Team Leader, UAV Navigation - Grupo Oesia, San Sebastián de los Reyes (Madrid), Spain. [jmpulido@uavnavigation.com](mailto:jmpulido@uavnavigation.com)
- José Manuel Torrente Delgado** Navigation Engineer, UAV Navigation - Grupo Oesia, San Sebastián de los Reyes (Madrid), Spain. [jmtorrente@uavnavigation.com](mailto:jmtorrente@uavnavigation.com)
- Javier Bernal Urbaneja** Navigation Engineer, UAV Navigation - Grupo Oesia, San Sebastián de los Reyes (Madrid), Spain. [jbernal@uavnavigation.com](mailto:jbernal@uavnavigation.com)
- Antonio Alejandro Aslan Suárez** Navigation Engineer, UAV Navigation - Grupo Oesia, San Sebastián de los Reyes (Madrid), Spain. [aaaslan@uavnavigation.com](mailto:aaaslan@uavnavigation.com)
- Pablo Chiva Ruiz** Navigation Engineer, UAV Navigation - Grupo Oesia, San Sebastián de los Reyes (Madrid), Spain. [pchiva@uavnavigation.com](mailto:pchiva@uavnavigation.com)

## ABSTRACT

This work presents a navigation architecture for unmanned aerial vehicles designed to ensure reliable performance in GNSS-denied environments. The proposed system integrates two complementary modules to achieve drift-free navigation under jamming and spoofing. The first module, the AD-AHRS, fuses inertial, magnetometer, and air data measurements to estimate attitude and predict position and velocity states. It also includes integrity monitoring to detect GNSS degradation and accepts corrections from the visual navigation module, which comprises four submodules: visual odometry, template matching, terrain reference navigation, and map matching. Visual odometry estimates velocity by tracking feature displacements across frames, while template matching enables position updates in mapped areas. When flying over regions not flown before, terrain reference navigation correlates digital elevation models with radar altimeter profiles to mitigate drift at low altitude, whereas at higher altitudes, map matching compares onboard imagery with satellite maps to obtain absolute position. Combining these methods yields a navigation solution robust to GNSS outages and cumulative drift. The paper describes the architecture, presents validation results from datasets, and reports flight tests conducted during Jammertest 2025 under intentional jamming and spoofing.

**Keywords:** GNSS-denied, sensor fusion, terrain reference, visual map matching, jamming and spoofing resilience

# Nomenclature

AD-AHRS	=	Air Data Attitude Heading Reference System
AGL	=	Above Ground Level
ASL	=	Above Sea Level
AOV	=	Angle Of View
DEM	=	Digital Elevation Model
DL	=	Deep Learning
GNSS	=	Global Navigation Satellite System
IMU	=	Inertial Measurement Unit
INS	=	Inertial Navigation System
ISR	=	Intelligence, Surveillance and Reconnaissance
MM	=	Map Matching
TRN	=	Terrain Reference Navigation
UAV	=	Unmanned Aerial Vehicle
VNS	=	Visual Navigation System
VO	=	Visual Odometry

## 1 Introduction

Global Navigation Satellite Systems (GNSS) have long been foundational for autonomous aerial navigation, providing precise position, navigation, and timing (PNT) information. However, in contested or adverse environments, GNSS signals remain vulnerable to intentional interference. Jamming consists of transmitting high-power noise or structured signals that overwhelm the legitimate satellite signals, effectively denying service. Spoofing involves the generation of counterfeit GNSS signals that emulate authentic ones, leading the receiver to compute erroneous estimates with potentially severe consequences. Meaconing [1], in contrast, captures genuine GNSS signals and re-transmits them with delay or modification, thereby shifting the perceived time or position without creating fully synthetic signals. With the increasing availability of low-cost interference devices and software-defined radios, these threats are no longer confined to laboratory demonstrations but have become realistic risks to operational systems [2].

In light of these threats, it is imperative that flight control systems do not rely solely on GNSS but instead integrate a diverse set of onboard sensors and estimation techniques to maintain robustness and availability under all flight conditions. The proposed architecture in this paper follows a multi-layer fusion strategy: starting from classical inertial navigation enhanced with air data inputs to improve baseline performance, the system mitigates drift by incorporating terrain reference navigation and absolute visual localization by comparing onboard images with satellite maps. This layered approach enables the UAV to sustain accurate navigation in GNSS denied environments.

The remainder of the paper describes the architecture in detail, beginning with the AD-AHRS module, followed by the visual navigation system and its submodules, and then presents preliminary results obtained using terrain reference navigation and map matching. Finally, results from flight campaigns conducted during the Jammertest 2025 are reported and discussed.

## 2 Air-Data Heading Reference System Architecture

The nucleus of the architecture obtains attitude estimation at a high rate using three-axes accelerometers and gyroscopes, and three axes magnetometers. Then, the outside loops of the navigation system aim to obtain the estimated position and velocity by fusing the barometric pressure sensor, dynamic



pressure sensor and outside air temperature sensor. The correction source can either come from the GNSS receiver, or from the Visual Navigation System. The AD-AHRS monitors continuously the GNSS receiver variables and compares it with the rest of the observables to detect the presence of interference. When jamming or spoofing are detected, the VNS data comes into place. The block diagram of how the architecture works is represented in Figure 1.

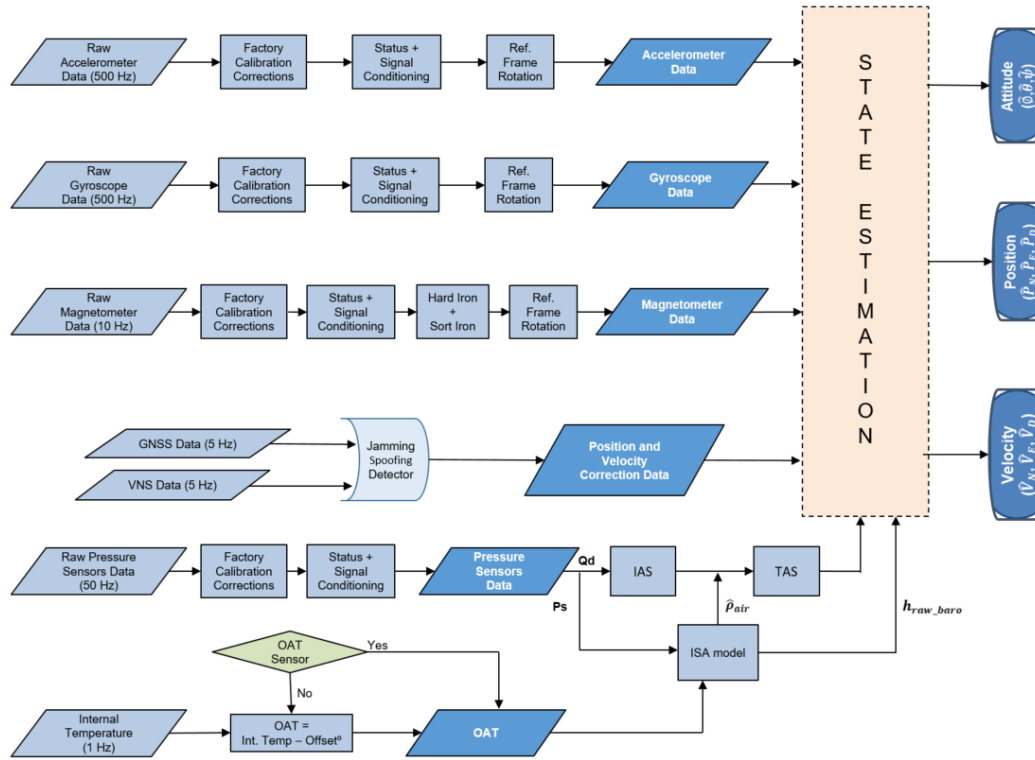


Fig. 1 AD-AHRS state estimation logics

### 3 Visual Navigation System Architecture

The VNS module operates as an independent component that primarily relies on computer vision techniques to mitigate the drift inherent to dead-reckoning navigation. It features a complex internal architecture and provides low-frequency position and velocity corrections to the state estimation module within the AD-AHRS, thereby enhancing overall robustness in GNSS-denied scenarios. Each of its submodules is tailored to specific flight conditions and in some cases requires the availability of additional sensors. By complementing one another, these submodules ensure that the system remains sufficiently robust to provide reliable navigation estimates under a wide range of flight conditions.

#### 3.1 Visual Odometry and Template Matching

Visual odometry is a technique that computes the displacement of the aircraft by comparing the singular points of two consecutive camera frames. It provides a velocity correction source but accumulates a small error over time, approximately a 1% of the traveled distance. This submodule is available as long as there is enough luminosity and the velocity and AGL of the aircraft are convenient to let the camera take two images that have features in common.

Template matching is a technique used to store significant features of an image together with their associated coordinates. It requires knowledge of the actual location where the reference image was captured, and to achieve full error correction the area must first be overflowed with GNSS available. The method relies on feature detectors and descriptors to match the stored images with those acquired by the

onboard camera [3]. Algorithms such as RANSAC or KD-Tree are then employed to efficiently identify the reference image that best corresponds to the current view and to infer the associated coordinates. A map of a previously surveyed area can be reused provided that the flight altitude is similar to that at which the reference map was generated; in practice, the valid range extends from half to twice the original above-ground level (AGL).

### 3.2 Terrain Reference Navigation and Map Matching

Terrain Reference Navigation is an advanced geolocation technology based on comparing the overflow terrain morphology with previously stored topographic maps. The objective is to identify similarities and accurately estimate the aircraft's position. An elevation profile is generated from altimeter measurements acquired by onboard sensors and correlated with a DEM to determine the most probable position [4]. Thus, the algorithm monitors in real time the difference between the DEM profile and the ground level computed from the estimated altitude and the altimeter measurement. The search area is determined by calculating a weighted average of a correlation coefficient, the offset between both signals, and their standard deviation. The local maxima within the search area are used to estimate the position error provided by the algorithm [5], which is then converted into Cartesian displacement to obtain a position estimate in latitude and longitude. The algorithm must be executed periodically to ensure that the distance between consecutive samples does not become too large, allowing it to correctly compute the confidence level.

The performance of this technique is strongly conditioned by several factors. First, it depends on the characteristics of the overflow terrain: flat areas lack distinctive features for reliable correlation, while highly irregular relief can introduce radar measurement errors due to multipath reflections or mismatches with the DEM. Second, the measurement strategy plays a critical role, since insufficient sampling or spacing reduces the fidelity of elevation profiles, whereas denser sampling increases computational load. In addition, the reliability of the altitude data, both AGL and ASL, is crucial, as errors caused by sensor noise, false returns, or adverse weather directly degrade the algorithm's accuracy. Finally, aircraft dynamics also affect measurement quality, as turbulence or aggressive maneuvers can distort the topographic profile and compromise correlation performance. This technique is ideal for low-altitude flight missions.

The Map Matching technique is based on matching images taken onboard with the georeferenced database based on satellite maps to compute the aircraft position. The technique uses a DL model which mainly contains a feature extractor, a correlation module, and an iterative homography estimator [6]. The algorithm needs to process the satellite image in order to scale it and match the onboard camera image. When flying higher, each pixel represents a larger ground area. This adjustment is computed in real time, and by knowing the AGL, AOV, and the resolution of the satellite image, the image can be cropped. Figure 2 represents the mathematical relation between each of the previous terms.

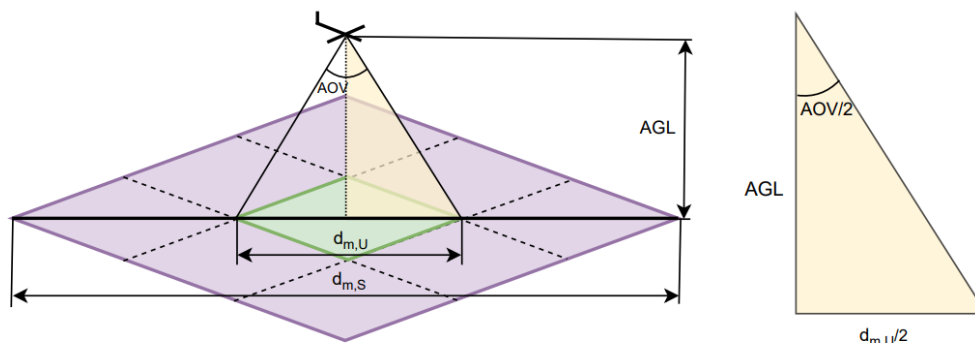


Fig. 2 MM image scale adjusting

The main challenges come with the difference in illumination, resolution, and perspective of the images compared. The images could also be taken in different seasons or the landscape might have changed. To cover a wide variety of scenarios, the DL model used was pretrained using the Boson-nighttime dataset [7], which contains both thermal and daylight images. Flying over very homogeneous places like oceans or deserts is also a challenge. This technique is ideal for higher-altitude flight missions.

## 4 Results

### 4.1 Post-processing dataset

The last two functionalities are currently being integrated into the standard product, and a high-fidelity simulator has been developed that can process real flight datasets and imagery to execute the algorithms. Figure 3 illustrates the results obtained with the TRN algorithm during a long trajectory.

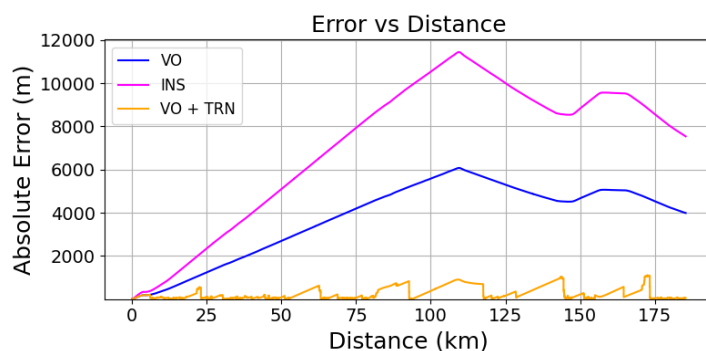


**Fig. 3 TRN error over travelled distance.**

The blue curve represents the absolute position error (in meters) between the true position and the estimate derived from only using visual odometry; the pink curve corresponds to the INS solution; the orange curve shows the absolute position error with the solution obtained fusing VO and TRN. It can be seen that the error is completely cancelled when the algorithm finds a new solution. For a 187 km trajectory with TRN active, the system achieved an average absolute error of  $239 \pm 16$  m, which corresponds to a 0.1 % of the travelled distance.

Figure 4 represents some results using the MM algorithm using an actual flight dataset of a 36 km trajectory. It compares the improvement that this algorithm implies, since navigating only with INS implies a 4% error with respect to travelled distance, and visual odometry around 1%. When using MM the error is limited to an error of  $31 \pm 9$  m, which represents 0.08 % error with respect to travelled distance.

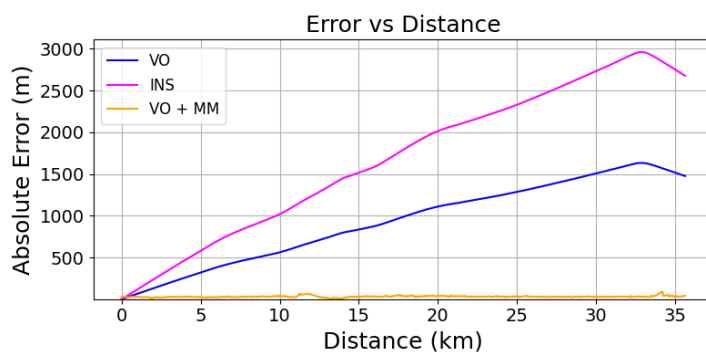


**Fig. 4 Map Matching error over travelled distance.**

Taking a look at the 2D coordinate plot with an actual flight trajectory, Figure 5 represents the comparison of the ground truth vs the solution provided by each of the algorithms. The ground truth is represented in red; the blue dotted line contains the VO-only solution; the pink dotted represents the INS solution; the green crosses represent the points where a new solution from TRN/MM algorithms is found; and the orange line contains the fusion of VO + each of the algorithms. The results show that both algorithms allow to fly in GNSS-denied environments during trajectories in order of kilometers with less than 50 meters of error at the end of the trajectory.

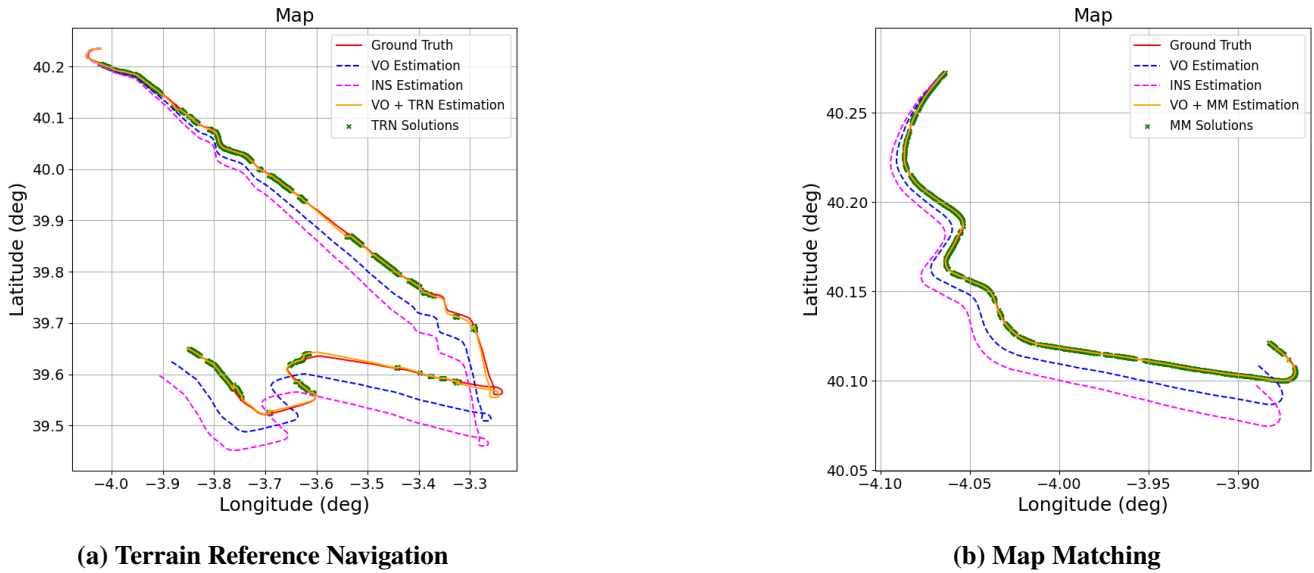


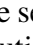
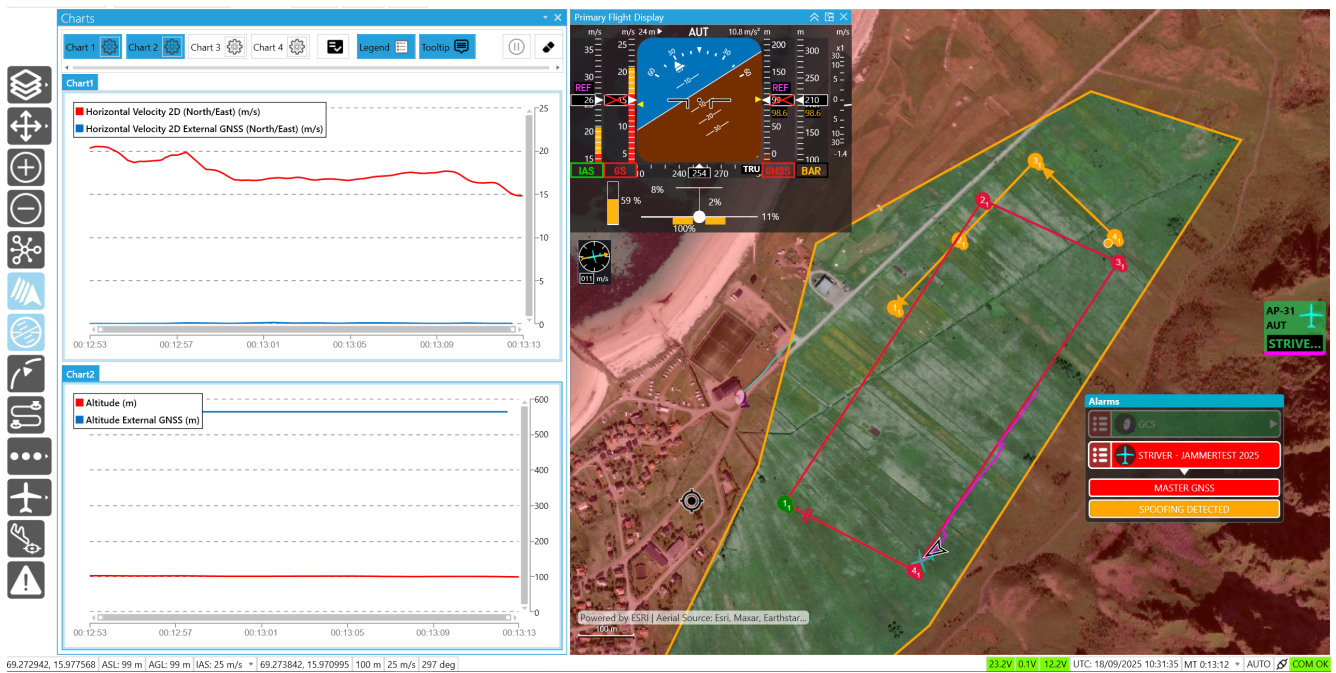


Fig. 5 Ground truth trajectory versus TRN and MM submodules.

## 4.2 GNSS-denied flight testing

The architecture including the AD-AHRS, visual odometry, and template matching algorithms has been evaluated in real jamming/spoofing conditions, taken place at Jammertest 2025. The flight control solution has been installed in a 10 kg electric VTOL able to fly in the range 15-30 m/s. The first protection layer comes with detecting the GNSS-denied conditions on time, so that the flight control solution never jumps into a false GNSS PNT. The test corresponds to number 2.5.22 according to official transmissions manual [8], which consists on Signals GPS L1 C/A, L2C, L5, Galileo E1, E5, E6 where there are 5 minutes of initial jamming (L1, G1, BQI, L2, E5b, L5 with 2W) prior to spoofing transmission, then continuous on other bands than the ones spoofed. The spoofed position has fixed coordinates.

Figure 6 contains a snapshot taken at the ground control software when the attack is active. It can be seen that a static attack is being transmitted, where the altitude is fixed to 570 m and the speed is almost null. The broadcasted GNSS position is represented with the  icon, the VNS position is seen as , while the position from the sensor fusion is . The mission represents an example of ISR operation, where a common flight plan is continuously followed. As it can be seen, the AD-AHRS triggers the spoofing detected warning, and takes out GNSS from its navigation solution. The aircraft was able to keep on flying without deviating its trajectory for the rest of the flight thanks to using the template matching algorithm.



**Fig. 6** Spoofing flight test at Jammertest 2025

## 5 Conclusion

This paper has presented a robust navigation architecture developed by UAV Navigation - Grupo Oesia for operating in GNSS-denied environments, integrating an AD-AHRS with a multi-modal visual navigation system. The combination of visual odometry, template matching, terrain reference navigation, and map matching enables the system to mitigate drift and provide reliable position and velocity estimates under jamming and spoofing conditions. Post-processing of real dataset studies and flight test campaigns, including Jammertest 2025, have demonstrated the architecture's capability to detect and isolate GNSS degradations while sustaining accurate navigation over extended distances. Results show that drift can be effectively bounded below 0.1 % of the travelled distance. Ongoing work focuses on further integration of TRN and MM modules into the standard product and on extending the validation campaigns to more challenging environments.

# Declaration of Use of Artificial Intelligence

Artificial intelligence tools were employed solely to check grammar, enhance readability, and improve the clarity of the text in previously written sections. These tools were not used to generate scientific content, formulate answers to the presented research problems, or interpret experimental results. The authors have carefully reviewed and edited all AI-assisted text as needed and take full responsibility for the content of this publication.

## References

- [1] Ali Broumandan, Ali Pirsiavash, Isabelle Tremblay, and Sandy Kennedy. Evaluation of NovAtel’s jamming and spoofing detection and mitigation capabilities during Jammertest2024. In *Proceedings of the 2025 International Technical Meeting of The Institute of Navigation*, pages 401–413, Long Beach, California, Jan. 2025. doi: [10.33012/2025.20012](https://doi.org/10.33012/2025.20012).
- [2] Katarina Radoš, Marta Brkić, and Dinko Begušić. Recent advances on jamming and spoofing detection in GNSS. *Sensors*, 24(13), 2024. ISSN: 1424-8220. doi: [10.3390/s24134210](https://doi.org/10.3390/s24134210).
- [3] Christine Van Kirk, Alice Chen, Saad Biaz, and Richard Chapman. Dead reckoning and terrain image processing as basis for UAV home-oriented navigation under foreign GPS-denied environments. *Journal of Computing Sciences in Colleges*, 38:74–89, 2022.
- [4] Taeyun Kim, Seongho Nam, Hyungsub Lee, and Juhyun Oh. Verification of vision-based terrain-referenced navigation using the iterative closest point algorithm through flight testing. *Sensors*, 25(18), 2025. ISSN: 1424-8220. doi: [10.3390/s25185813](https://doi.org/10.3390/s25185813).
- [5] Juhyun Oh, Chang-Ky Sung, Jungshin Lee, Sang Woo Lee, Sang Jeong Lee, and Myeong-Jong Yu. Accurate measurement calculation method for interferometric radar altimeter-based terrain referenced navigation. *Sensors*, 19(7), 2019. ISSN: 1424-8220. doi: [10.3390/s19071688](https://doi.org/10.3390/s19071688).
- [6] Jihong Xiao, Ning Zhang, Daniel Tortei, and Giuseppe Loianno. STHN: Deep homography estimation for UAV thermal geo-localization with satellite imagery. *IEEE Robotics and Automation Letters*, 9(10):8754–8761, 2024. doi: [10.1109/LRA.2024.3448129](https://doi.org/10.1109/LRA.2024.3448129).
- [7] Jihong Xiao and Giuseppe Loianno. UASTHN: Uncertainty-Aware Deep Homography Estimation for UAV Satellite-Thermal Geo-localization, 2025. <https://arxiv.org/abs/2502.01035>.
- [8] Jammertest Consortium. *Jammertest 2025 Test Catalogue*, 2025.

